AFRL-RZ-WP-TP-2009-2210

ROLLING CONTACT FATIGUE LIFE AND SPALL PROPAGATION CHARACTERISTICS OF AISI M50, M50 NiL, AND AISI 52100, PART III–METALLURGICAL EXAMINATION (PREPRINT)

Nelson H. Forster, Lewis Rosado, William P. Ogden, and Hitesh K. Trivedi

Mechanical Systems Branch
Turbine Engine Division

OCTOBER 2009

STINFO COPY

AIR FORCE RESEARCH LABORATORY
PROPULSION DIRECTORATE
WRIGHT-PATTERSON AIR FORCE BASE, OH 45433-7251
AIR FORCE MATERIEL COMMAND
UNITED STATES AIR FORCE

REPORT DOCUMENTATION PAGE

1. REPORT DATE *(DD-MM-YY)*	2. REPORT TYPE	3. DATES COVERED *(From - To)*
October 2009	Journal Article Preprint	01 May 2006 – 01 May 2008

4. TITLE AND SUBTITLE

ROLLING CONTACT FATIGUE LIFE AND SPALL PROPAGATION CHARACTERISTICS OF AISI M50, M50 NiL, AND AISI 52100, PART III–METALLURGICAL EXAMINATION (PREPRINT)

5a. CONTRACT NUMBER
In-house

5b. GRANT NUMBER

5c. PROGRAM ELEMENT NUMBER
62203F

6. AUTHOR(S)

Nelson H. Forster and Lewis Rosado (AFRL/RZTM)
William P. Ogden (Pratt & Whitney)
Hitesh K. Trivedi (UES, Inc.)

5d. PROJECT NUMBER
3048

5e. TASK NUMBER
06

5f. WORK UNIT NUMBER
304806IH

7. PERFORMING ORGANIZATION NAME(S) AND ADDRESS(ES)

Mechanical Systems Branch (AFRL/RZTM)
Turbine Engine Division
Air Force Research Laboratory, Propulsion Directorate
Wright-Patterson Air Force Base, OH 45433-7251
Air Force Materiel Command, United States Air Force

Pratt & Whitney
East Hartford, CT

UES, Inc.
Dayton, OH 45432

8. PERFORMING ORGANIZATION REPORT NUMBER
AFRL-RZ-WP-TP-2009-2210

9. SPONSORING/MONITORING AGENCY NAME(S) AND ADDRESS(ES)

Air Force Research Laboratory
Propulsion Directorate
Wright-Patterson Air Force Base, OH 45433-7251
Air Force Materiel Command
United States Air Force

10. SPONSORING/MONITORING AGENCY ACRONYM(S)
AFRL/RZTM

11. SPONSORING/MONITORING AGENCY REPORT NUMBER(S)
AFRL-RZ-WP-TP-2009-2210

12. DISTRIBUTION/AVAILABILITY STATEMENT

Approved for public release; distribution unlimited.

13. SUPPLEMENTARY NOTES

Journal article submitted to the Society of Tribologists and Lubrication Engineers.

PAO Case Number: 88ABW-2008-3138, 21 Jun 2008. Paper contains color.

The U.S. Government is joint author of this work and has the right to use, modify, reproduce, release, perform, display, or disclose the work.

14. ABSTRACT

This is the third part of a three-part series which investigates the rolling contact fatigue initiation and spall propagation characteristics of three bearing materials, namely AISI 52100, VIM-VAR M50, and VIM-VAR M50 NiL steels. While there is substantial prior work published on the rolling contact fatigue initiation of these materials, little is known about their spall propagation characteristics after spall initiation. In Part III, 208 size, 40 mm bore bearings are examined for changes in appearance of the microstructure; as well as residual stress as a function of depth in the circumferential direction. Correlations between experimental results from Part I and computer modeling in Part II are made.

15. SUBJECT TERMS

rolling element bearings, rolling contact fatigue life, bearing metallurgy and microstructure

16. SECURITY CLASSIFICATION OF:			17. LIMITATION OF ABSTRACT:	18. NUMBER OF PAGES	19a. NAME OF RESPONSIBLE PERSON (Monitor)
a. REPORT Unclassified	**b. ABSTRACT** Unclassified	**c. THIS PAGE** Unclassified	SAR	34	Garry D. Givan **19b. TELEPHONE NUMBER** *(Include Area Code)* N/A

i

Rolling Contact Fatigue Life and Spall Propagation Characteristics of AISI M50, M50 NiL, and AISI 52100, Part III - Metallurgical Examination

Nelson H. Forster
Lewis Rosado
Propulsion Directorate
Air Force Research Laboratory
Wright-Patterson Air Force Base, Ohio 45433

William P. Ogden
Pratt & Whitney
East Hartford, CT

Hitesh K. Trivedi
UES Inc.
Dayton, Ohio 45432

ABSTRACT

This is the third part of a three-part series which investigates the rolling contact fatigue initiation and spall propagation characteristics of three bearing materials, namely AISI 52100, VIM-VAR M50, and VIM-VAR M50 NiL steels. While there is substantial prior work published on the rolling contact fatigue initiation of these materials, little is known about their spall propagation characteristics after spall initiation. In Part III, 208 size, 40 mm bore bearings are examined for changes in appearance of the microstructure; as well as residual stress as a function of depth in the circumferential direction. Correlations between experimental results from Part I and computer modeling in Part II are made.

INTRODUCTION

The gas turbine industry is pursuing material technology to meet mainshaft bearing needs of future engines. Past bearing material programs typically used the bearing fatigue life as the primary measure of performance i.e., the time until the material initiates a fatigue spall. However, there is also a desire to understand what happens after initiation of the spall. It is during this period when the bearing is liberating material that bearing failures in the field are detected, usually from the spalled material collected on the magnetic chip detector. The objective of the research described in Part III of this paper is to investigate changes in the microstructure of the bearing steel that occur in the loaded ball track, as well as the leading edge of the spall front. In Part I, Rosado [1] showed that AISI M50 and M50 NiL bearings tested had much longer fatigue life and longer propagation times to reach the same level of damage under the same Hertzian contact stress as the AISI 52100 bearings tested. In Part II, Arakere [2] showed that the subsurface von Mises stresses are sufficient for significant plastic yielding to occur at the spall edges due to reduced contact area and impact loading. The plastic yielding from impact was sufficient to cause significant changes in the residual stress of the material. In Part III, we are examining the microstructure of the steel for insight into the effect of alloy content, residual stress, Hertzian stress, and impact stress on the microstructure and ultimately bearing life and propagation rate. By doing so, it may provide engineers guidance on how to increase life and decrease the spall propagation rate, improving reliability of bearings in the field.

Alteration in the microstructure of 52100 bearing steel from rolling contact is well documented in the literature [3-10]. These studies primarily used metallurgical sectioning, polishing, etching and optical microscopy to examine a dark etching region (DER) occurring in the subsurface region of 52100 bearings. Generally, the material examined was from highly loaded bearings which ran at least 10^6 cycles. The DER is attributed to microstructural changes and occurs as a band of fairly uniform appearance at a depth of 0.10 to 0.60 mm [3]. The darker color is due to the transformed material being more susceptible to the etchant. Swahn provides several detailed micrographs of this phenomenon and shows the emergence of the DER is affected by the number of stress cycles and magnitude of the applied stress for 52100 bearing steel. The appearance of the DER is also affected by the heat treatment as noted by Martin [4] who showed that a 52100 bearing tested in a similar manner as Bush [5] did not display the DER. Martin suggested the reduction in retained austenite, as a result of tempering temperature, is responsible for the absence of the DER in the bearings he tested. It is also noted by Swahn and others that with sufficient cycles, white etching bands (WEB) will emerge in the DER followed by loss of hardness as measured by Vickers microhardness indenter. Martin detected WEB without the formation of the DER, suggesting these two phenomena are independent.

Voskamp [6-9] has extensively studied the rolling track of 52100 bearings from highly loaded life testing using x-ray diffraction. The bearings tested by Voskamp were 52100 steel, heat treated to a martensitic structure, and tempered at 150°C for one hour. The bearings tested by Voskamp contained up to 10 vol

% retained austenite after tempering [8]. After testing, Voskamp noted the formation of residual compressive stress in the circumferential and axial direction and residual tensile stress in the radial direction. Voskamp credited the formation of the residual stress to micro-plastic deformation with only secondary contributions from the transformation of retained austenite to martensite [9, p 107]. He also utilized his observations of residual stress in 52100 bearings to explain bearing life. Central to Voskamp's explanation of bearing life is that the formation of the residual stress occurs in three distinct stages: Stage I - Involves yield, micro-plastic deformation, and work hardening of the material which occurs during the first 1,000 revolutions of operation [9, p 61]; Stage II – The work hardened material has steady state behavior and resists further plastic micro-deformation, the bearing spends much of its life in this stage and the duration is strongly dependent on loading and temperature conditions [9, pp 61-63]; Stage III – The material undergoes distinct micro-deformation leading to phase transformation, further changes in residual stress, and softening in the subsurface of the loaded zone. The probability of crack initiation leading to fatigue failure increases due to an increase in the subsurface volume that is plastically deformed and residual tensile stresses that are formed due to plastic deformation [9, pp 182-183]. Voskamp concluded that for bearings to fail (spall) in rolling contact fatigue, they must enter this third and final stage. This approach to bearing life is quite different than the Lundberg-Palmgren (L-P) life theory which is based on the probability of an inclusion in the loaded zone propagating a crack. In the L-P model, bearing life is predetermined by the condition of the

4

steel from the time the bearing was made. With Voskamp, the history of the bearing operating condition plays a major role in bearing fatigue life.

While there are numerous papers on microstructural alterations with 52100 bearings there is very little on this phenomena with M50 and M50 NiL materials commonly used in the aviation gas turbine engine industry. However, one such study was conducted by Braza [10].   In a manner similar to this paper, Braza investigated the microstructure and residual stress of M50, M50 NiL, and 52100 bearings after high load testing. Braza noted that alteration in the microstructure is a long life, high stress event, seldom observed in service. However, service failures do occur and are generally initiated at surface defects. At these localized sites, stresses may be high enough to induce microstructural damage, even in highly alloyed materials such as M50. This is similar to the rationale in our current study, in which we are interested in how the increased stress at the edge of the spall affects the microstructure. Braza found WEB, high compressive stress, and softening in 52100; localized micro-structural damage known as 'butterflies', work hardening, but no appreciable loss of hardness in M50; no 'butterflies' but a different type of WEB was found in M50 NiL. Braza attributed the microstructural changes in 52100 as a thermo-mechanical tempering type of reaction and attributed less damage in M50 and M50 NiL to higher alloy content and secondary hardening that helps stabilize the microstructure.

EXPERIMENTAL

Test Bearings

The bearings analyzed in this study are 208 size (40 mm bore) bearings. The bearings with M50 and M50 NiL races had Si_3N_4 rolling elements and silver plated 4340 cages. The bearings with 52100 races had 52100 rolling elements and cotton-phenolic cages. The 52100 bearings analyzed were commercial-off-the-shelf bearings intended for machine tool spindles. The 52100 bearings were air melt/vacuum degassed and tempered at 200^oC. The M50 and M50 NiL bearings were made to standards used for aviation engine bearings. The M50 and M50 NiL bearings were vacuum induction melted-vacuum arc remelted and tempered three times at 540^oC and 525^oC respectively.

The bearings listed in Table 1 were first life tested and then tested for propagation. Some of the bearings in Table 1 developed a spall during the life testing, while others were the companion bearings and are suspensions. If the bearing developed a spall, the initial spall is the propagation site. For the suspended bearings, a series of four Rockwell C indents were used as the spall initiation site. The life testing portion of the test was performed at 3.10 GPa maximum Hertzian stress on the inner race. The test housing was heated to maintain a bearing outer race temperature of 131^oC. The oil inlet temperature was 99^oC and the measured oil scavenge temperature was approximately 121^oC. The oil flow to each bearing was 1.5 liters per minute. The conditions for the propagation testing were similar to the life testing except the load was reduced to produce an inner race maximum Hertzian stress of 2.41 GPa and the test head

band heaters were lowered in temperature to produce an outer race temperature of 110°C. The length of the propagation test was determined by mass loss predicted by an oil debris monitor. The limit for mass loss is roughly 100 mg, which produces a spall approximately 50 mm long on the bearing inner race.

In addition, a few new bearings were analyzed in which the spalls were initiated from Rockwell C hardness indents made with a 150 kg load. Table 2 lists the specific bearings studied that were initiated from indents without first life testing. New bearings of each material were also evaluated as a baseline. Additional details are provided in Part I regarding bearing geometry and test conditions.

X-Ray Diffraction Analysis

Residual compressive stress measurements were made on the bearings in the circumferential direction using x-ray diffraction (XRD) in accordance with SAE HS-784 [11]. The specific bearings examined are labeled "XRD' in the Post Test Analysis column of Tables 1 and 2. Measurements were made in the ball track at the spall front (direction of propagation) and approximately 180° degrees away from the middle of the spalled region. Measurements were made at the surface and nominal depths of 13, 25, 51, 76, 127, 178, 254, 381,508, and 762 µm. The material was removed electrolytically for subsurface measurement in order to minimize alteration of the subsurface residual stress.

Retained austenite measurements were made on the surface and at nominal depths of 127 and 254 µm depths. These measurements were made at

the same location as the residual stress measurements that correspond to these nominal depths. Volume percent retained austenite values were calculated from the "R" ratios and the total integrated intensities of the austenite (200) and (220), and the ferrite/martensite (200) and (211) diffraction peaks.   Four measurements were made at each site for statistical averaging.

Micro-Structural Analysis and Hardness Measurement

Selected 40mm bore inner rings were examined post test for microstructure and microhardness. The specific bearings examined are labeled 'microstructure' in the Post Test Analysis column of Tables 1 and 2. The inner races were initially cross sectioned in the radial direction immediately after the spall site (in the direction of spall propagation) and approximately circumferentially opposite to examine the material in the rolling track away from the spall. Then, a second cut was taken to expose the subsurface in the circumferential direction. All specimens were etched with 4% nitric acid in methanol prior to examination. Hardness measurements were made using a Vickers indenter with a 300 gm load on various optically different microstructure areas and then converted to Rockwell C values.

RESULTS

X-Ray Diffraction Analysis

The circumferential stress distributions measured as a function of depth for untested 40 mm bearing races are shown graphically in Figure 1. All of the

materials show high compressive stress at the immediate surface due to finishing of the bearing. Both M50 and 52100 are through hardened materials, so the residual compressive stress below 10 microns is essentially nil. M50 NiL is a case carburized material with intentional residual compressive stress to improve fatigue life. This particular bearing has a residual stress of 400 MPa to a depth greater than 0.50 mm, which is typical for this material and size of bearing. The depth of the carburized layer is set to insure the maximum value for the von Mises, orthogonal, and shear stress occurs well within region of high residual compressive stress.

The residual compressive stress of bearing 1000B after spall propagation testing is shown in Figure 2. The material is 52100. The bearing inner race completed 1.5×10^6 cycles at 3.10 GPa to produce the initial spall from indents. The bearing completed an additional 5.85×10^6 cycles during propagation to obtain a spall approximately 50 mm long in the rolling direction.   The profile indicates a significant residual compressive stress of 600 MPa at a depth of 0.13 mm at the spall edge and a slight dip to 100 MPa in the rolling track away from the spall. The shallower depth and higher level near the spall edge may be due to ball impact forces which would cause higher subsurface shear stress closer to the surface than the normal rolling stress. Both traces also show compressive stress near the surface that is deeper than expected for finishing. This is possibly due to the initial deformation from run in.

Residual stress profiles for bearing 075B are shown in Figure 3. The bearing is made from M50 steel and the spall was initiated from indents. The

bearing operated at 3.10 GPa for 75.1×10^6 cycles for initiation and 187×10^6 cycles at 2.41 GPa to propagate the spall. The bearing shows compressive stress attributed to plastic deformation near the surface at the edge of the spall. The region away from the spall does not show a significant difference relative to the stress profile of the material in a new bearing. Apparently, there are enough stress cycles to alter the residual stress near the spall, but not in the rolling track away from the spall.

Residual stress profiles for bearing 215 are shown in Figure 4. The bearing is made from M50 steel and the spall was initiated from indents after suspension from life testing. The bearing accumulated 16×10^9 cycles at 3.10 GPa during life testing and an additional 31×10^6 cycles during propagation testing. The bearing shows a residual compressive stress dip at 0.13 mm at the edge of the spall which roughly corresponds with the predicted depth to the maximum von Mises stress during the propagation test. The magnitudes and depths to maximum von Mises and shear stresses are covered in more detail in Part II. For bearing 215, the residual stress magnitude is higher near the spall; 657 MPa, compared to 461 MPa away from the spall, indicating there is more plastic deformation occurring at the spall edge than in the ball track. This is also covered in more detail in Part II.

Residual stress profiles for bearing 046B are shown in Figure 5. The bearing is made from M50 NiL steel and the spall was initiated from indents after suspension from life testing. The bearing operated for 19×10^9 cycles at 3.10 GPa during life testing and 17×10^6 cycles at 2.41 GPa during the spall

10

propagation testing. The results show that accumulated cycles contribute additional residual compressive stress in the circumferential direction beyond what is imparted during heat treatment. Adjacent to the spall, the maximum residual stress of 611 MPa occurs at a depth of 0.14 mm. Away from the spall, the maximum residual stress is about 657 MPa and occurs at a depth of 0.25 mm.

The mean volume percent of retained austenite (RA) was measured for all of the bearings in Tables 1 and 2. Measurements were made at the surface and at nominal depths of 0.13 and 0.26 mm. In general, the new 52100 showed RA levels of 1.4 ± 0.3, 2.0 ± 0.3, and 1.9 ± 0.5 % by volume at depths of surface, 0.13 mm, and 0.25 mm, respectively. This is much lower than most of the 52100 bearings previously tested, except for those tested by Martin. The new M50 bearings had the lowest RA of 0.5 ± 0.2, 0.2 ± 0.3, 0.1 ± 0.1 %, measured at depths of 0.12 mm and 0.25 mm, respectively. The new M50 NiL material ranged from 1.4 ± 0.5, 2.8 ± 0.7, 2.9 ± 1.2 % at depths of 0.12 mm and 0.26 mm. In general, there was no noticeable loss of RA in all of the bearings from high cycle loading, regardless of time or location relative to the spall. The results indicate that the small amount of RA in these bearing is not converted to untempered martensite as reported by others; therefore loss of RA cannot be used as a predictor of remaining bearing life for the materials tested here.

Microstructural Analysis and Hardness Measurement

The micrograph in Figure 6 is from 52100 bearing 221B. The micrograph shows a white etching region (WER) that occurs subsurface in the ball track. The appearance is different than the DER seen by Swahn and others but the location in the subsurface is similar. Generally white etching vs. dark etching suggests the material is more responsive to the etchant vs. less responsive. Martin found WEB without the DER in 52100 bearings that contained low retained austenite. The 52100 bearings in this study also had low retained austenite. The results indicate that changes have occurred to the material in the region of maximum shear stress and that the level of retained austenite may affect the formation of classic DER reported in 52100.

The micrograph in Figure 7 is from M50 bearing 074A. The micrograph shows a classic 'butterfly'. The appearance of butterflies is attributed to stress transformations that initiate at carbides or inclusions, which act as locations of increased stress intensity. Osterlund [12] determined that the butterflies are extremely fine grained ferrite and carbide from the decomposition of martensite, formed under rolling contact conditions. Aside from the butterflies, which were found in several locations, there was no other noticeable microstructural damage in this bearing.

The micrographs in Figures 8(a-c) are from bearing 216. This is an M50 bearing that was suspended after 4,267 hours in the life test. The region shown is taken near the spall location. Figure 8(a) is from the plane normal to the circumferential direction. Figures 8(b) and 8(c) show the plane normal to the axial direction at different magnifications. There is clear evidence of WEB.

12

Similar to 52100, the bands are oriented at two distinct angles. However, where Swahn found WEB at 80° and 30^0 relative to circumferential rolling direction (3), these bands are oriented 110° and 30° with the same reference orientation. Clearly there is microstructural decay occurring in this 'high time' M50 bearing and the decay is more significant than the 'low time' bearing 074A where the spall was initiated from indents.

No microstructural damage was found in the M50 NiL bearings examined, including bearing 045 B which had 5×10^{10} cycles. It is believed the residual compressive stress of M50 NiL helps delay the occurrence of micro-structural damage. However, this is different than what Braza reported for M50 NiL bearings.

Figures 9 shows an example of the hardness measurements conducted on bearing 216. This is the only bearing which showed any measureable loss of hardness. Converting Vickers to Rockwell C, the average hardness with standard deviation in the top layer was 62.6 ± 0.26; in the middle region with WEB the hardness was 60.2 ± 0.40; and in the subsurface 62.9 ± 0.93. In comparison the top layer for 52100 bearing 221 was 62.9 ± 0.41, 62.5 ± 0.16 in the middle region, and 62.2 ± 0.27 in the subsurface. The M50 showed a loss of 2 points in the WEB and no measureable loss was detected in several 52100 or M50 NiL specimens. That no loss of hardness was detected in the 52100 bearing was surprising in light of what Braza and others have reported. It may be related to the amount of retained austenite in the bearings, which was much lower in our 52100 bearings. The rationale for this is covered in the Discussion.

DISCUSSION

In Part I it was shown that 52100 bearing steel has significantly lower fatigue life than M50 or M50 NiL at an applied stress of 3.10 GPa (450 ksi) and outer race bearing temperature of $140^{\circ}C$ ($284^{\circ}F$); L10 = 151 x 10^6 vs. 16601 and 3051 x 10^6, respectively. In this paper it is shown that 52100 undergoes significant changes in residual stress and microstructure in the range of 10^6 to 10^7 cycles with the applied test conditions. M50 showed evidence of butterfly formation and higher residual at the spall edge, but no noticeable change in the regions we examined away from the spall at 10^7 cycles. The 52100 steel in these test was vacuum degassed but not vacuum melted. Also the 52100 bearings have different internal geometry and metal balls compared to silicon nitride balls used in the M50 and M50 NiL bearings. The mass difference between a steel rolling element and silicon nitride rolling element will alter the impact stress and it is expected this will affect the propagation rate. However, the impact loading is separate of fatigue initiation. It is hard to explain the difference in rolling contact fatigue life of 52100 compared to M50 based on 'cleanliness' of the steel. Additional studies of metal ball vs. silicon nitride should be conducted on both 52100 and M50 to separate the effect of ball density on the propagation rate.

Significant microstructural damage in the form of WEBs was found in the high time M50 bearings with 10^9 cycles. In Part I it was shown that M50 bearings with high operation time propagated faster than new bearings with spalls initiated from indents, suggesting correlation with higher microstructural damage in the high-time M50 bearings. Also, there was little change in residual stress in the ball track of M50 at 10^6 cycles but substantial change at 10^9 cycles. M50 seems to follow Voskamp's finding for 52100 that significant plastic deformation occurs at the end of the useful life leading to microstructural alterations, i.e., Stage III of the bearing life. However, M50 appears to require 10^3 times more cycles to enter this phase than the 52100 steel tested here.

That no damage was found in M50 NiL bearings at 10^{10} cycles is interesting. It was also shown in Part I that the spall propagation of M50 was faster in the high time bearings that in new bearings initiated from indents, but there was no noticeable change in propagation rate for the low and high time M50 NiL bearings. Perhaps the inherent residual stress of a case carburized material helps mitigate the micro-structural damage in M50 NiL and the propagation rate in low time and high time bearings remains the same.

It is also important to note that we were only able to measure residual stress in the circumferential direction. In this direction, and in the axial direction, residual stress from rolling contact plastic deformation is compressive. However, the resulting residual stress in the radial direction is tensile. Typical values measured by Voskamp on 52100 bearings are 500 MPa compressive in the circumferential direction at a depth of 0.25 mm [9, p93] and 300 MPa tensile in

15

the radial direction at a depth 0.12 mm [9, p 100]. We saw values of 600 MPa

and 650 MPa compressive stress in 52100 and M50 bearings near the spall edge

in the circumferential direction at depths of 0.13 mm. While we did not measure

the residual stress in the radial direction, it is likely that the magnitude of this

stress would be slightly over 300 MPa tensile at the spall edge for the 52100 and

high time M50 bearings. It is the residual tensile stress that is most damaging.

For the M50 NiL bearing, additional compressive stress of 600 MPa was found in

both the track away from the spall and at the spalls edge. This is 200 MPa

beyond the normal level of 400 MPa found in the untested M50 NiL bearing. The

radial stress in M50 NiL in these tested bearings is unknown, but the residual

compressive stress from heat treatment probably offsets the tensile stress

believed to be present in M50 and 52100.

That no evidence of DER was found in our 52100 bearings which had less

than 2% retained austenite supports Martin's hypothesis regarding the

connection of heat treatment and level of retained austenite to the formation of

the DER. Swahn postulated the DER structure to be ferrite with untempered

martensite, thermodynamically induced by cyclic rolling and diffusion of carbon

rather than thermal activation.   Braza found 9 points loss of hardness in the DER

on the Rockwell C scale for 52100 bearings initially containing 8 % austenite,

where as we found no appreciable loss of hardness for 52100 bearings initially

containing less than 2 % retained austenite and no formation of the DER. High

levels of retained austenite in new bearings seem to be responsible for the

formation of the DER and loss of hardness seen in prior tests with 52100 bearings.

There is also some useful information in this study regarding the mechanisms of bearing rolling contact fatigue life. In the time of the original Lundberg-Palmgren life model, inclusions were common in air melted 52100 bearing steel, so it was appropriate that the L-P life model be based on the statistical probability of an inclusion in the subsurface stress field of the bearing. Today steels are much cleaner. In service, it is much more likely for fatigue to initiate at the surface from small localized damage such as scratches rather than inclusions. Surface initiated fatigue was seen in Part I regarding the debris dents on M50 NiL from shedding of the TiN coating. In the absence of both inclusions and surface defects, the life seems to be determined by stability of the microstructure, which appears to be the life determining mode for 52100 and M50 bearings in this study.

CONCLUSIONS

The objective of the three part study was to look at the effects of alloy content and residual stress on the behavior of precision ball bearings in classical rolling contact fatigue and the propagation rate of spalls after initiation from rolling contact fatigue. The authors believe the additional alloy content in M50 is a critical factor in the improved performance over 52100. Consistent with the findings of Braza et al., the higher alloy content provides secondary hardening which helps stabilize the microstructure of M50 and M50 NiL relative to 52100.

However, additional studies should be performed to better separate the contributions for alloy content and the result of ball density, since this is a difference in the 52100 and M50 bearings tested in this study. The inherent residual compressive stress of M50 NiL seems to make this material more resistant to microstructural decay than M50. The inherent residual compressive stress likely offsets the formation of residual tensile stress in the radial direction which occurs in 52100 and M50. It was also shown in Part I that M50 bearings with 10^{10} cycles propagate faster than new M50 bearings with spall grown from indents. M50 NiL did not show this trend. We attribute the faster propagation rates in high time M50 bearings compared to M50 NiL to the formation of residual tensile stress in the radial direction and decay of the microstructure.

ACKOWLEDGEMENTS

REFERENCES

1. Rosado, L., Forster, N.H., Thompson, K., "On the Rolling Contact Fatigue Life and Spall Propagation Characteristics of M50, M50 NiL and 52100 Bearing Materials: Part I - Experimental Results," presented at 2008 STLE Annual Meeting and submitted for publication.

2. Nagaraj, A., Branch, N, Levesque, G., Svendsen, V., Forster, N.H., "On the Rolling Contact Fatigue Life and Spall Propagation Characteristics of M50, M50 NiL and 52100 Bearing Materials, Part II - Stress Modeling," presented at 2008 STLE Annual Meeting and submitted for publication.

3. Swahn, H., Becker, P.C., Vingsbo, O., "Martensite Decay During Rolling Contact Fatigue in Ball Bearings," Metallurgical Transaction, Vol 7A, 1976, pp 1099-1110.

4. Martin, J.A., Borgese, S.F. Eberhardt, A.D., "Microstructural Alteration of Rolling Bearing Steel Undergoing Cyclic Stressing," Trans. of the ASME, J. Basic Engineering, Vol 88, 1966, pp 555-567

5. Bush, J.J. and Grube, W.L., Robinson, G.H., "Microstructural and Residual Stress Changes in Hardened Steel Due to Rolling Contact," ASM Trans., Vol 54, 1961, pp 390-412.

6. Voskamp, A.P., Osterlund, R., Becker, P.C., Vingsbo, O., "Gradual Changes in Residual Stress and Microstructure During Contact Fatigue," Metals Technology, 1980, pp14-21.

7. Voskamp, A.P., "Fatigue and Material Response in Rolling Contact," <u>Bearing Steels: Into the 21st Century, ASTM STP 1327</u>, J.J.C. Hoo and W.B. Green Eds. American Society for Testing and Materials, 1998, 443-456.

8. Voskamp, A.P., "Microstructural Stability and Bearing Performance," <u>Bearing Steel Technology, ASTM STP 1419,</u> J.M. Besswick Ed., American Society for Testing and materials International, West Conshohocken, PA, 2002, pp 152-166.

9. Voskamp, A.P., "Microstructural Changes During Rolling Contact Fatigue," PhD Thesis, Delft University of Technology, Delft, The Netherlands, 1997, ISBN: 90-9010187-x.

10. Braza, J.F., Pearson, P.K., Hannigan, C.J., "The Performance of 52100, M-50, and M-50 NiL Steels in Radial Bearings," SAE Manuscript 932470, 1993, pp1-13.

11. Residual Stress Measurement by X-Ray Diffraction Measurement, Society of Automotive Engineers Publication HS-784, (2003).

12. Osterlund, R., Vingsbo, O., Vincent, L., Guiraldeng, P., "Butterflies in Fatigued Ball Bearings – Formation Mechanisms and Structure," Scandinavian Journal of Metallurgy, vol. 11 (1982) pp 23-32.

Table 1 - Bearings From Life Testing

Material	Bearing #	Life (Hours / 10^6 cycles @ 3.10 GPa)	Propagation (Hours / 10^6 cycles @ 2.41 GPa)	Post Test Analysis
52100	221B	Spall 131 / 599	1.6 / 7.3	Microstructure
52100	206B	Spall 5.4 / 24.6	5.9 / 26.9	XRD
M50	216	Suspension 4,267/ 16,343	0.3/1.3	Microstructure
M50	215	Suspension 4,267/ 16,343	7.9/31.0	XRD
M50 NiL	043B	Spall 1,436 / 5,500	2.8 / 10.72	Microstructure
M50 NiL	046B	Suspension 4,959 / 18,993	4.5 / 17.23	XRD
M50 NiL	045B	Suspension 4,959 / 18,993	6.3/24.9	Microstructure

Table 2 - New Bearings Spall Propagated From Indents

Material	Bearing #	Initiation (Hours / 10^6 cycles @ 2.41 GPa)	Propagation (Hours / 10^6 cycles @ 2.41 GPa)	Post Test Analysis
52100	1000B	0.36 / 1.50	1.4 / 5.85	XRD
M50	074A	10.3 / 39.4	19.4 / 74.3	Microstructure
M50	075B	19.6 / 75.1	48.9 / 187.3	XRD
M50NiL	036A	38.1 / 145.9	3.9 / 14.9	Microstructure
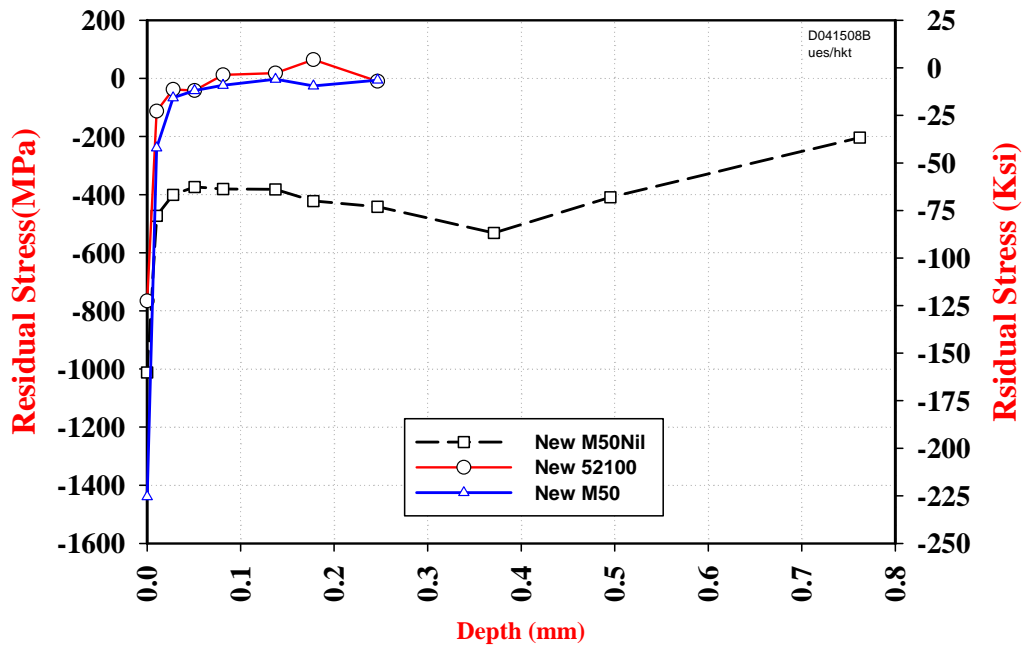
Figure 1. Residual stress profiles for untested material in the circumferential direction.
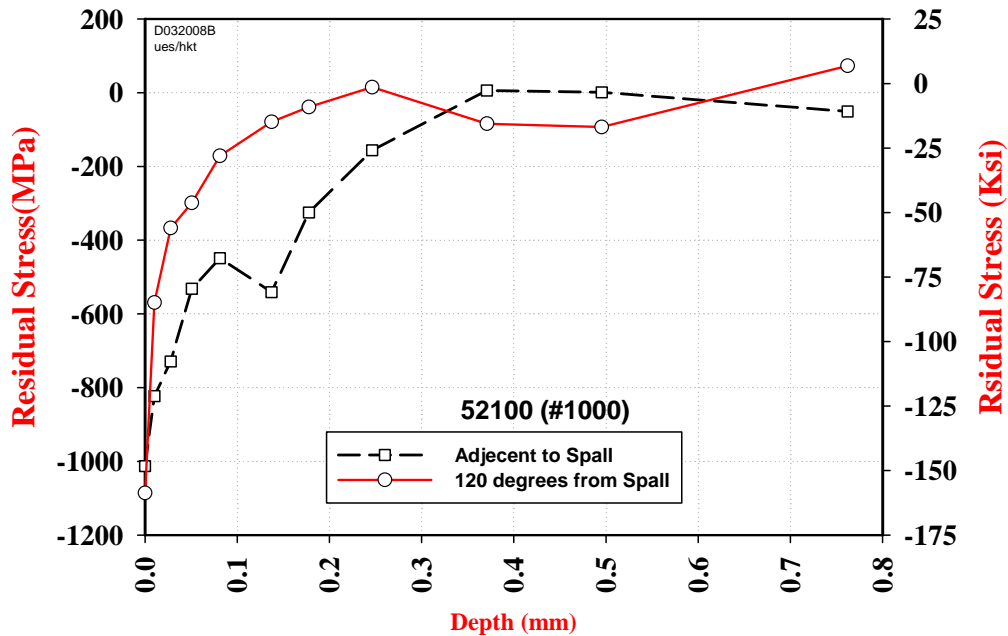
Figure 2. Residual stress measurements on bearing 1000B in the circumferential direction. This spall was initiated from indents. Propagation time 1.4 hours, 5.85 x 10^6 cycles.
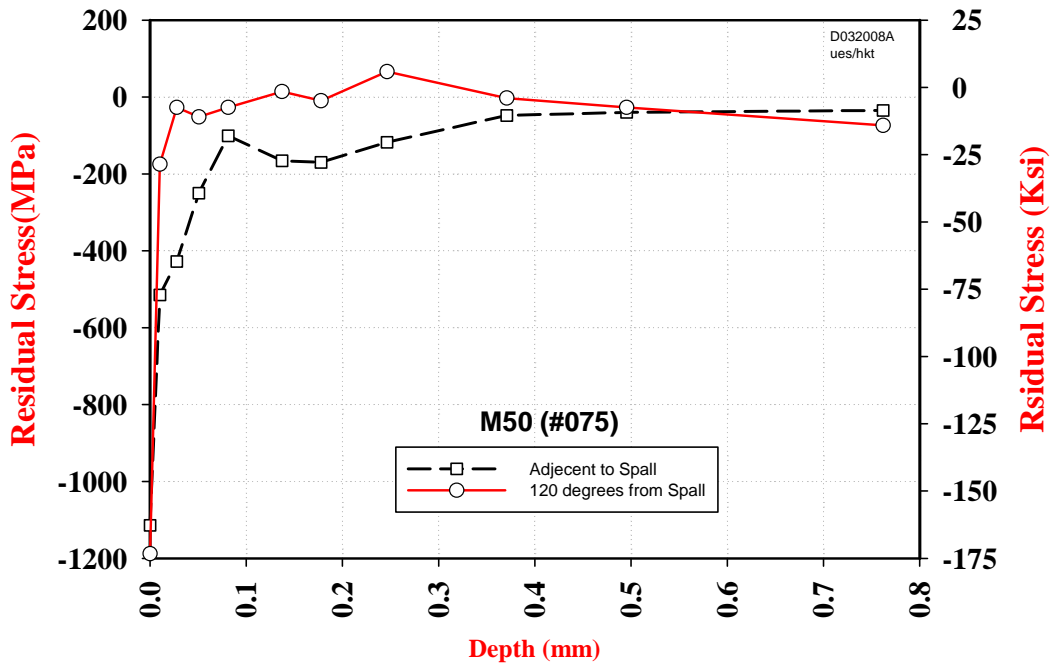
Figure 3. Residual compressive stress profile for M50 bearing No 075B in the circumferential direction. The spall was initiated from indents. Propagation time 48.9 hours, 187.3 x 10^6 cycles.
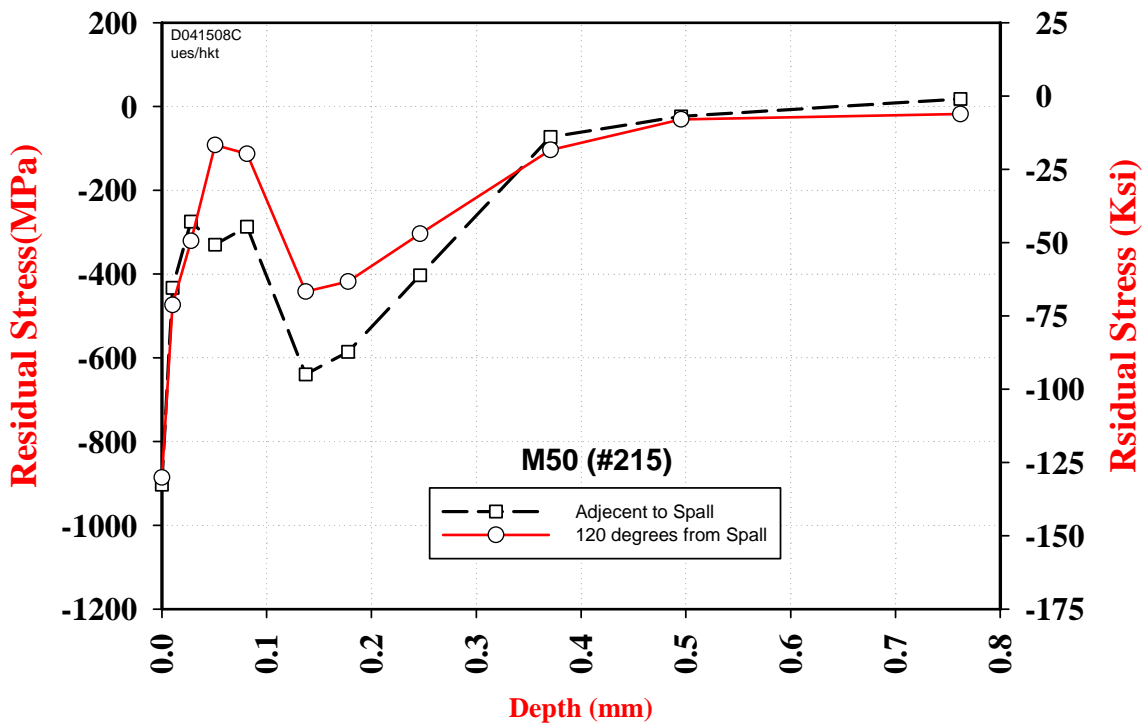

Figure 4. Residual compressive stress profile for long life M50 bearing. Life was 4,267 hours, 16 x 10^6 cycles. Propagation was 7.9 hours, 31 x 10^6 cycles.
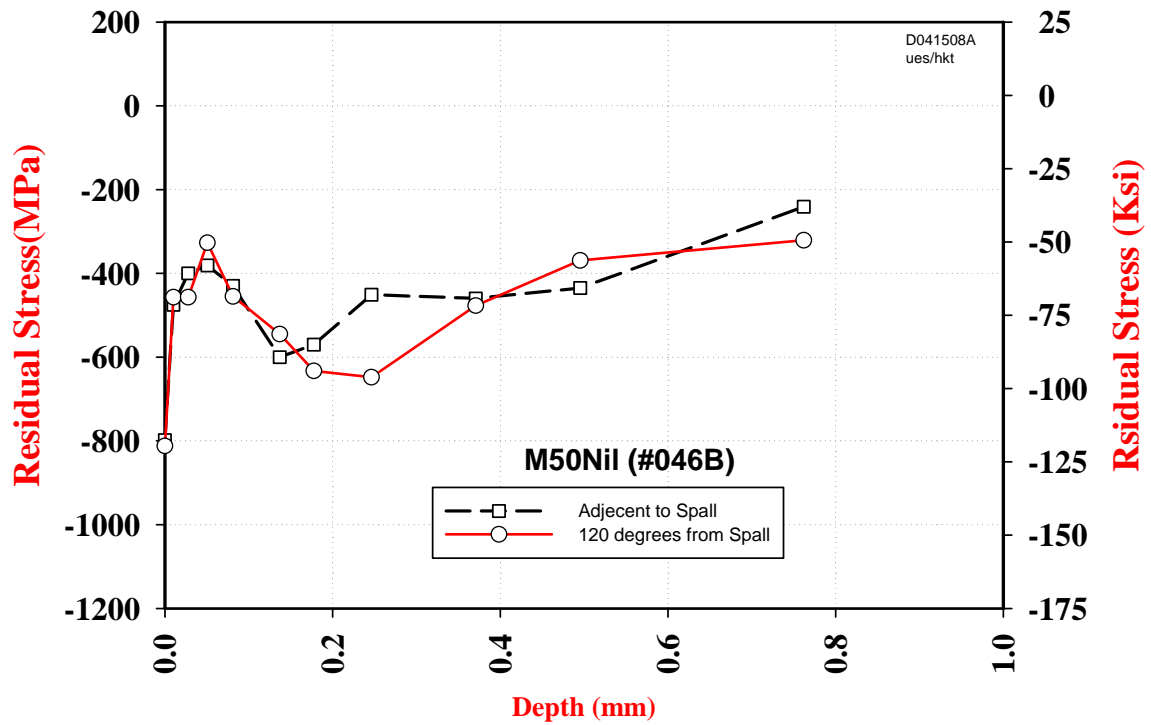
Figure 5. Residual compressive stress for long life M50 NiL bearing in the circumferential direction. Life was 4,959 hours, 19 x 10^6 cycles. Propagation was 4.5 hours, 17 x 10^6 cycles.
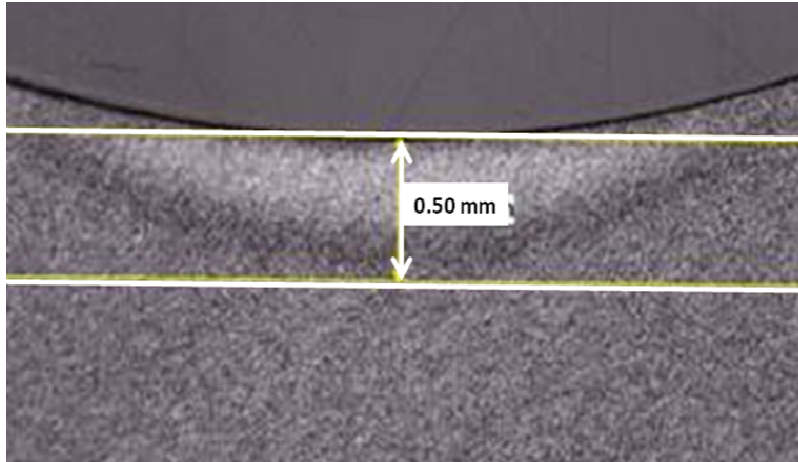
Figure 6. Micrograph of Bearing 221 B showing etching alterations in 52100 material. . Life was 131 hours, 599 x 10^6 cycles. Propagation was 1.6 hours, 7 x 10^6 cycles.
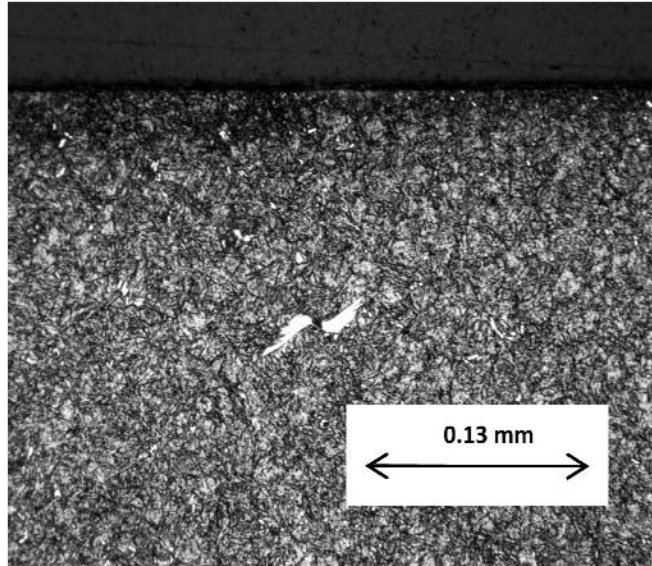

Figure 7. Micrograph of M50 Bearing 074A showing classic butterfly. New bearing spall propagated from indents. Propagation 19.4 hours, 74 x 10^6 cycles.
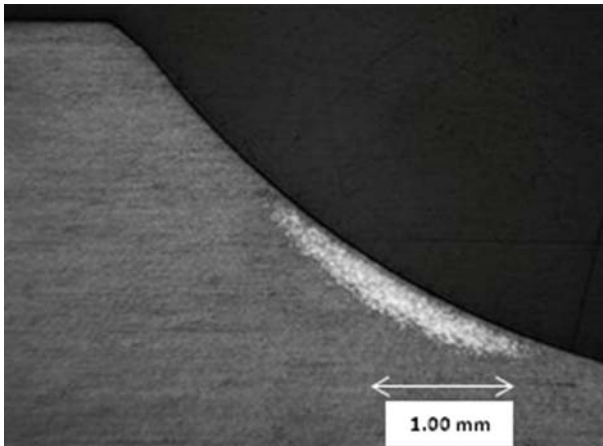
(a)
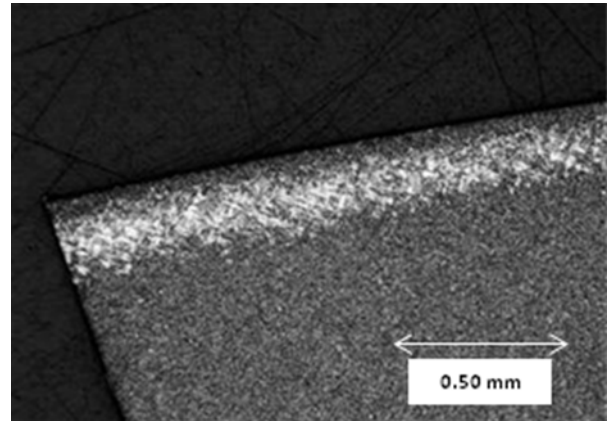
(b)
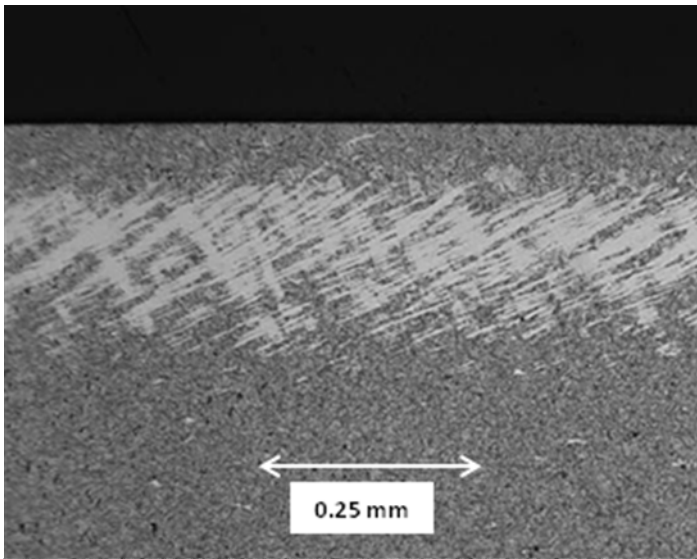
(c)

Figure 8. Cross section of M50 Bearing 216 slightly past the spalled area showing white etching band. (a) radial cross section (b) circumferential cross section (c) circumferential cross section at higher magnification. Life was 4,267 hours, 16 x 10^6 cycles. Propagation was 0.3 hours, 1.3 x 10^6 cycles.
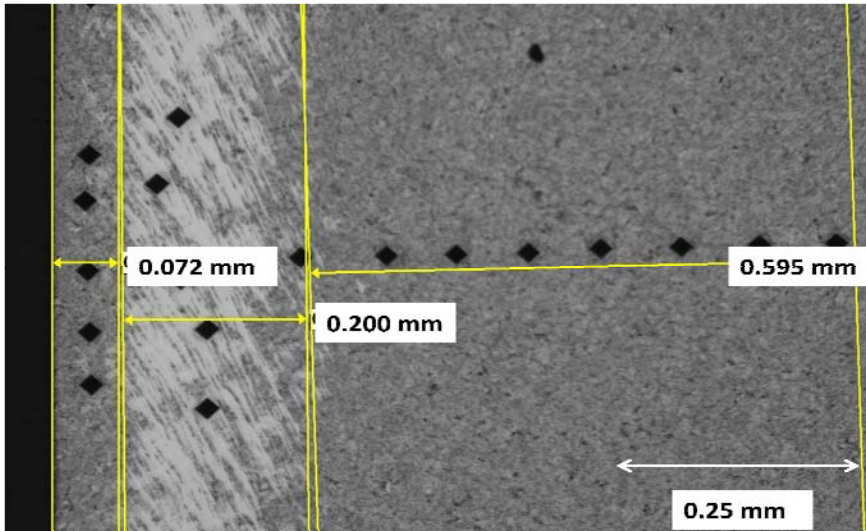
Figure 9. Hardness measurements on cross section of M50 Bearing 216.